/Construction of honey bee hives like CuO/PbO heterojunction photocatalysts with enhanced antibiotic and dye degradation activity under visible light

Karina Bano[a], Prit Pal Singh*[a], Sandeep Kumar[b], Shakir Mahmood Saeed[c], Saurabh Aggarwal[d], Ranvijay Kumar[e], Sandeep Kaushal[a,f]*

[a] Sri Guru Granth Sahib World University, Fatehgarh Sahib, Punjab, India

[b]Department of Chemistry, Akal University, Talwandi Sabo, Bathinda 151302, Punjab, India

[c] Department of Pharmacy, Al-Noor University College, Nineveh, Iraq

[d] Uttaranchal Institute of Technology, Uttaranchal University, Dehradun, India

[e]University Centre for Research and Development, Chandigarh University, Gharuan, Mohali, Punjab, India

[f]Regional Institute of Education, National Council of Educational Research and Training, Ajmer, Rajasthan, India

Address for Correspondence:
Prof. Prit Pal Singh
Sri Guru Granth Sahib World University, Fatehgarh Sahib, Punjab, India
E-mail: dhillonps2003@gmail.com

Dr. Sandeep Kaushal
Associate Professor
Regional Institute of Education, National Council of Educational Research and Training, Ajmer, Rajasthan, India

Email: kaushalsandeep33@gmail.com

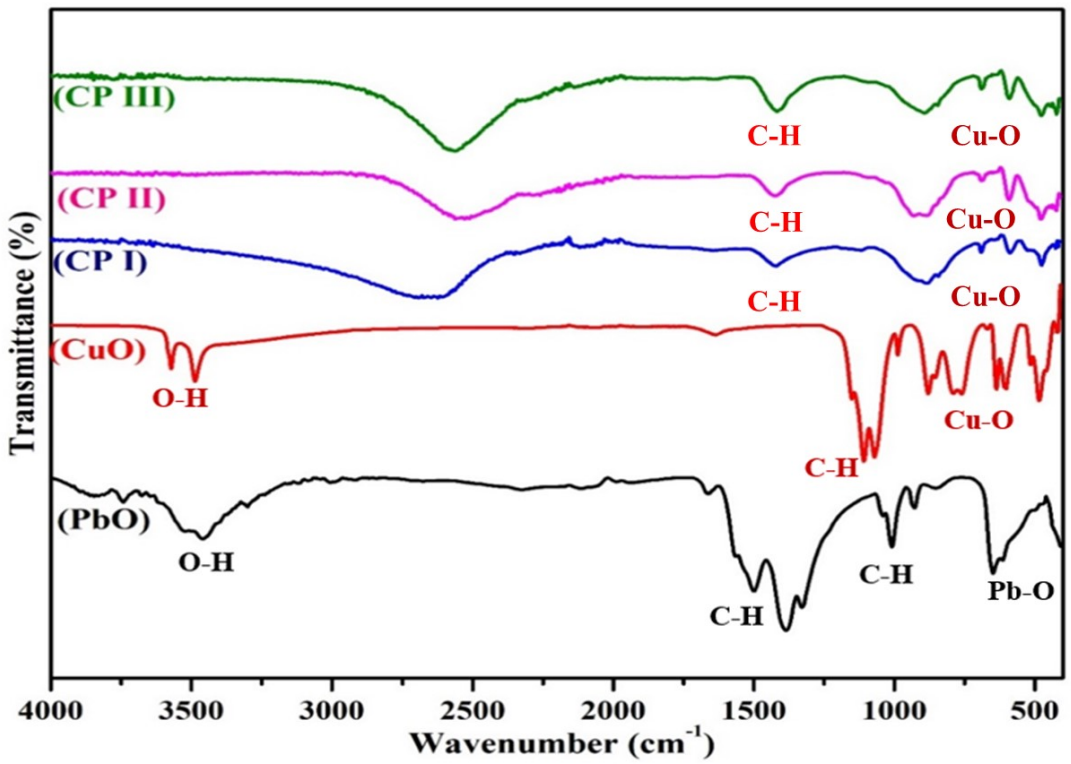

Fig. S1. FTIR spectrum of CuO, PbO and CuO/PbO heterojunction photocatalysts

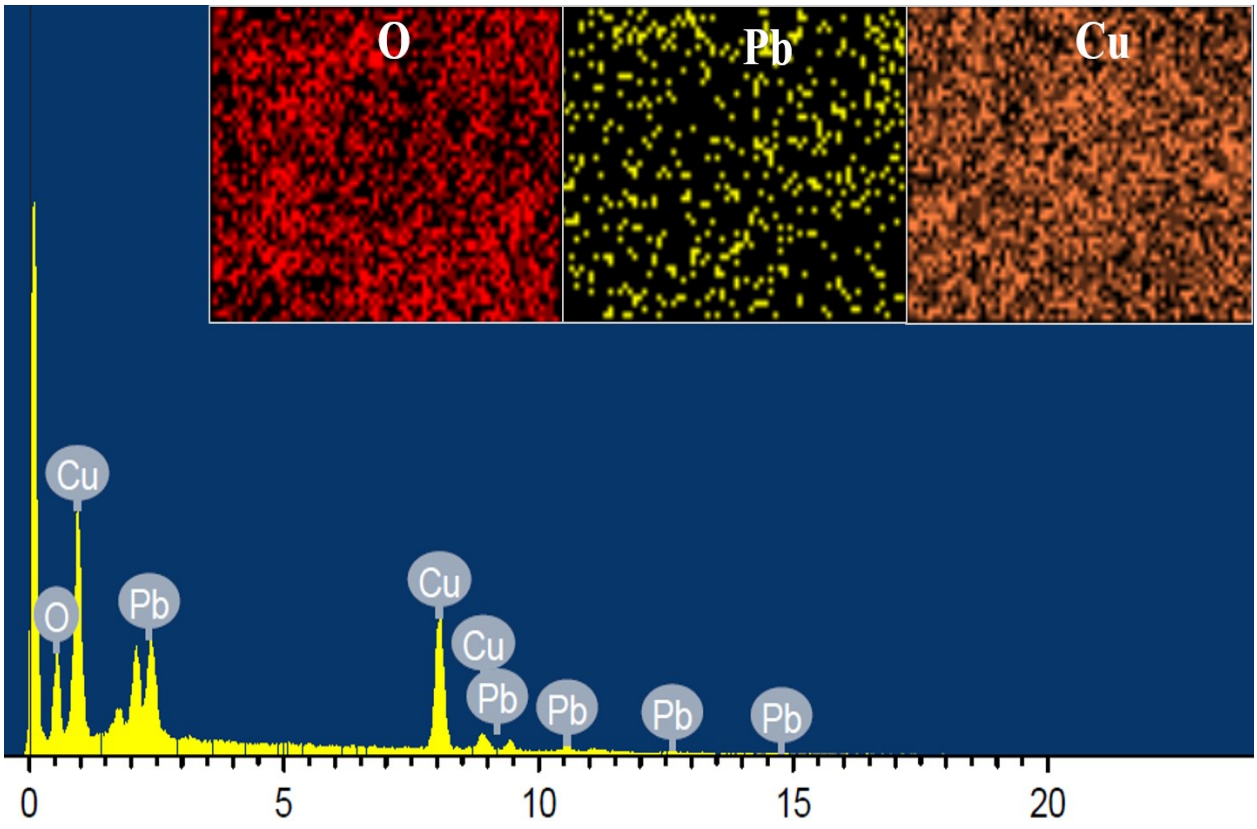

Fig. S2. EDS spectra and mapping of CuO/PbO heterojunction

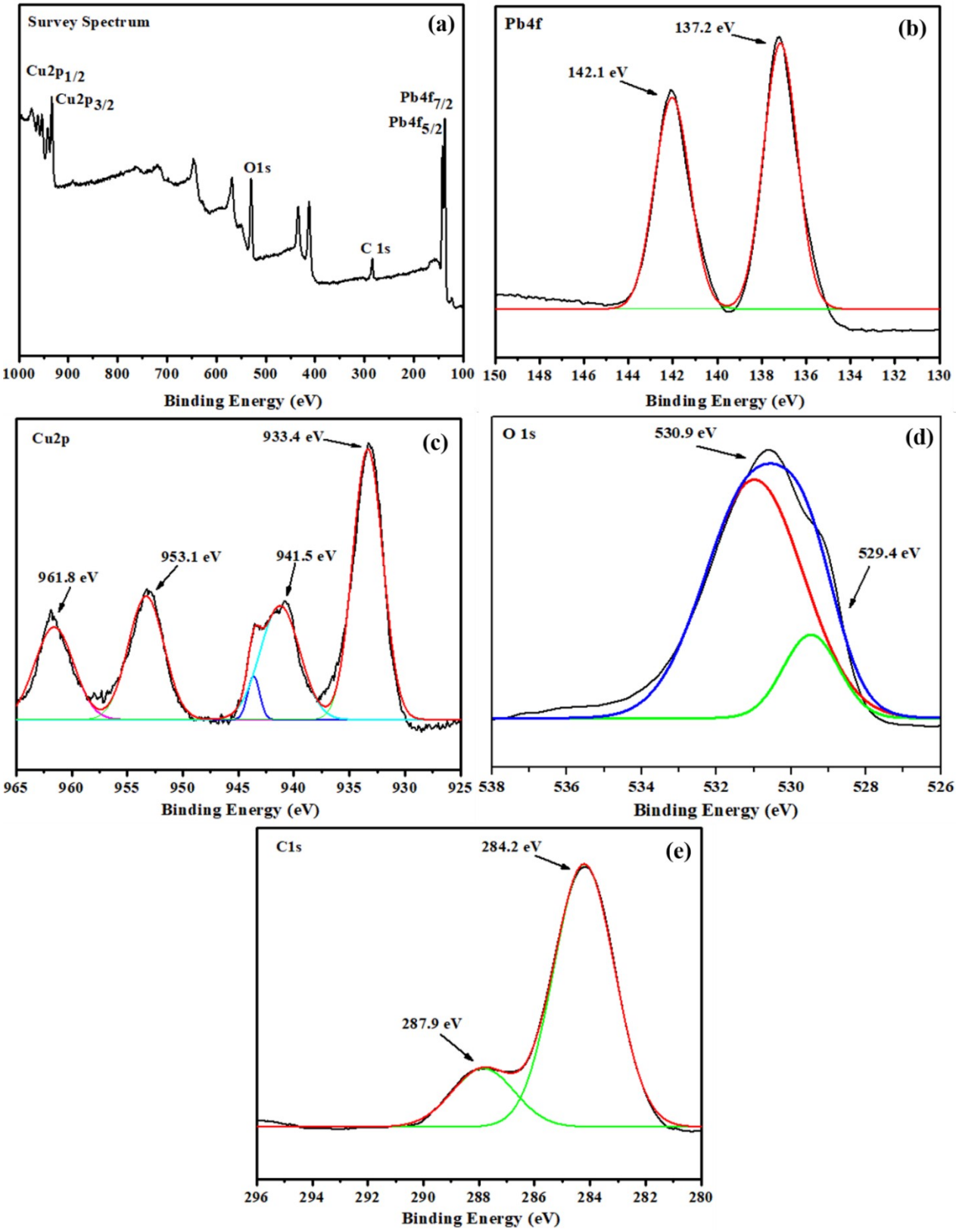

Fig. S3. XPS spectrum of CuO/PbO heterojunction.

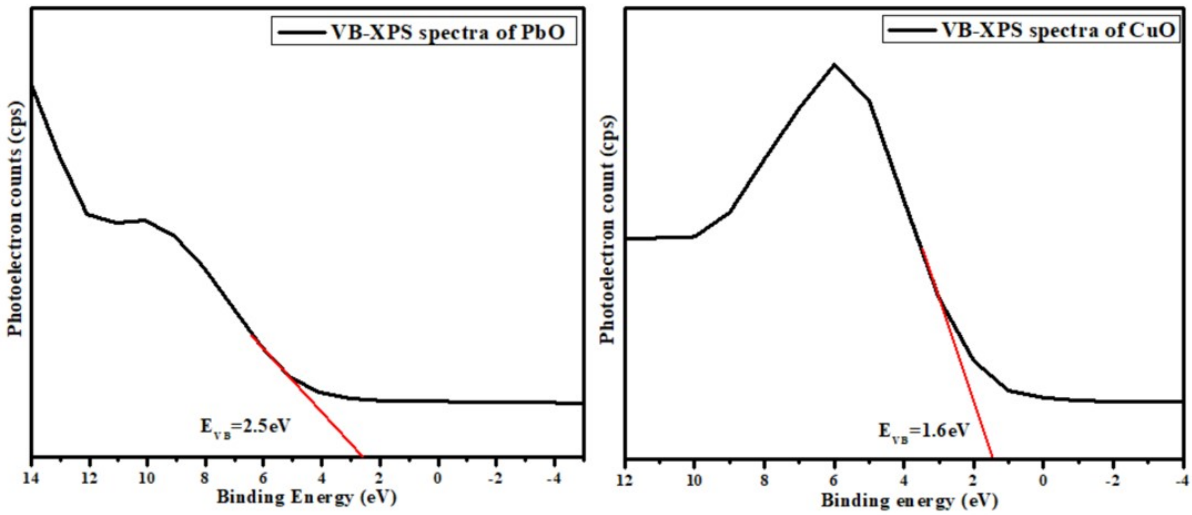

Fig. S4. VB-XPS spectra of PbO and CuO nanoparticles

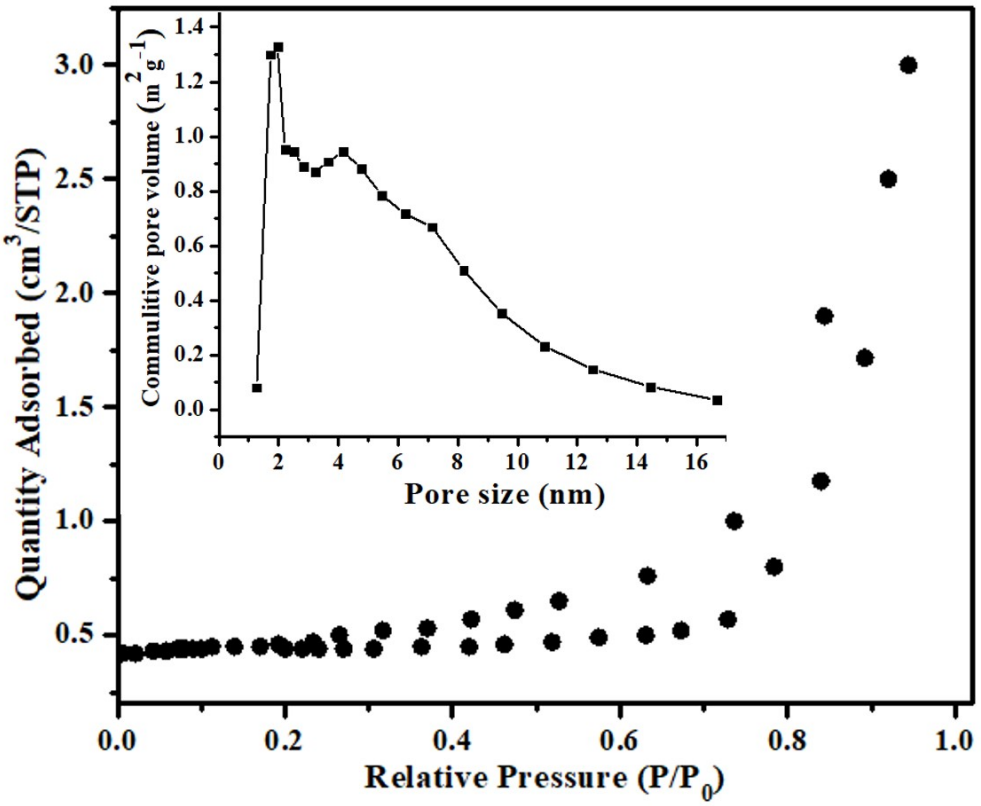

Fig. S5. Nitrogen adsorption–desorption isotherm (pore size distribution) for CuO/PbO heterojunction photocatalyst

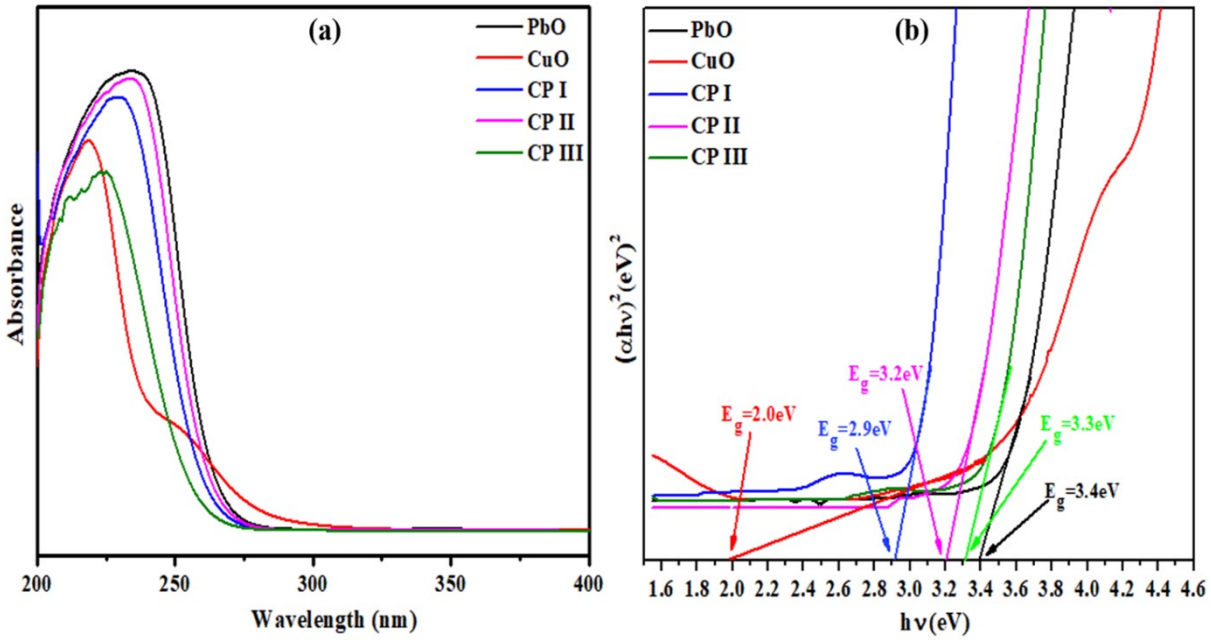

Fig. 6 Depiction of a) UV-Visible spectrum and b) tauc-plot band gap energy values of heterojunction photocatalysts

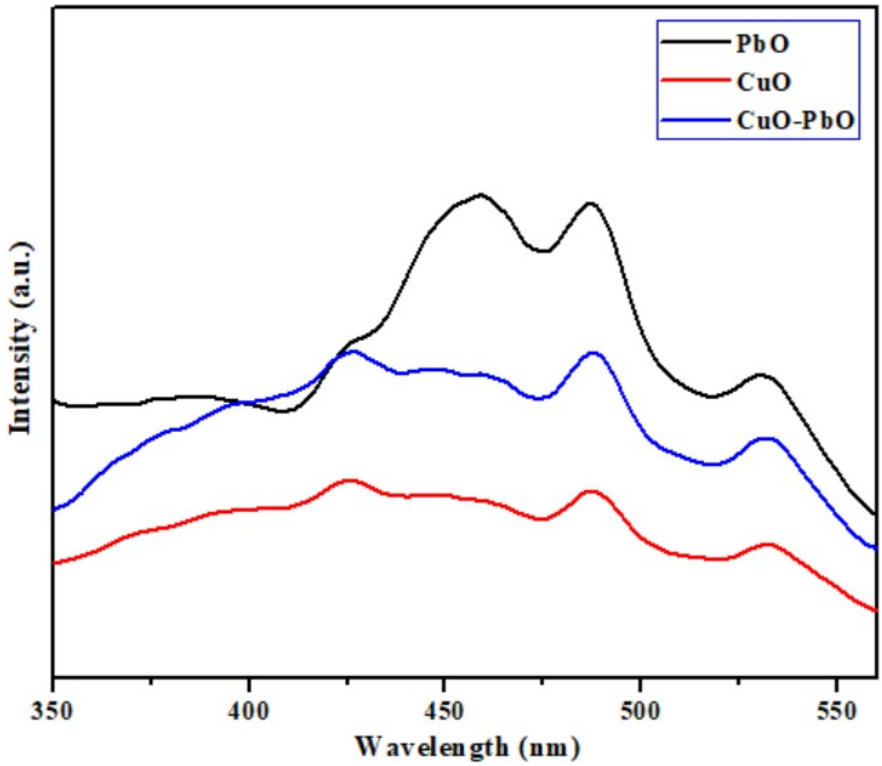

Fig. S7. PL spectrum of PbO, CuO semiconductors and CuO/PbO heterojunction photocatalyst

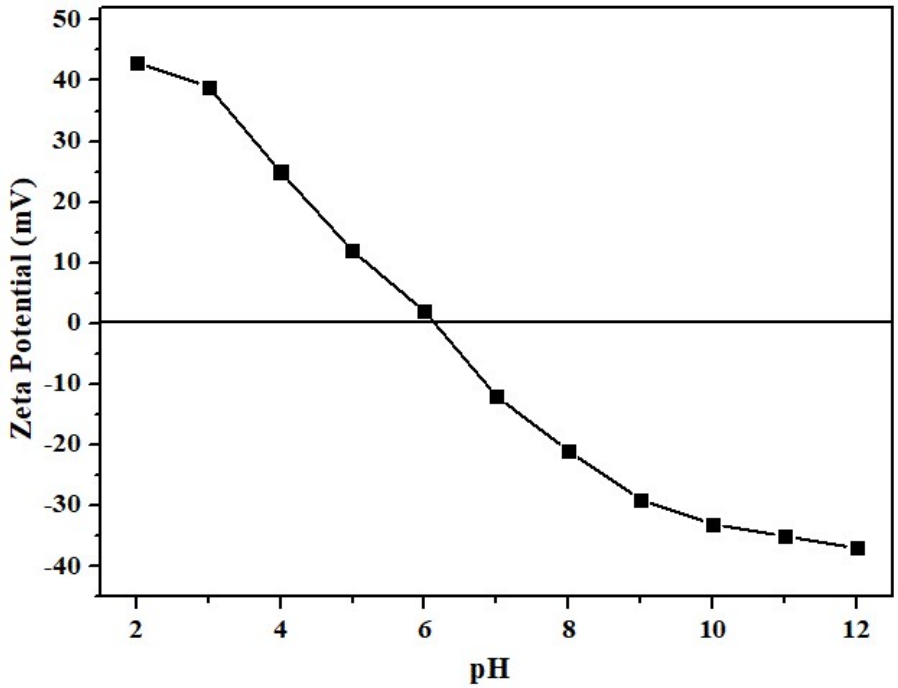

Fig. S8 Zeta potential of CuO/PbO heterojunction at different pH values

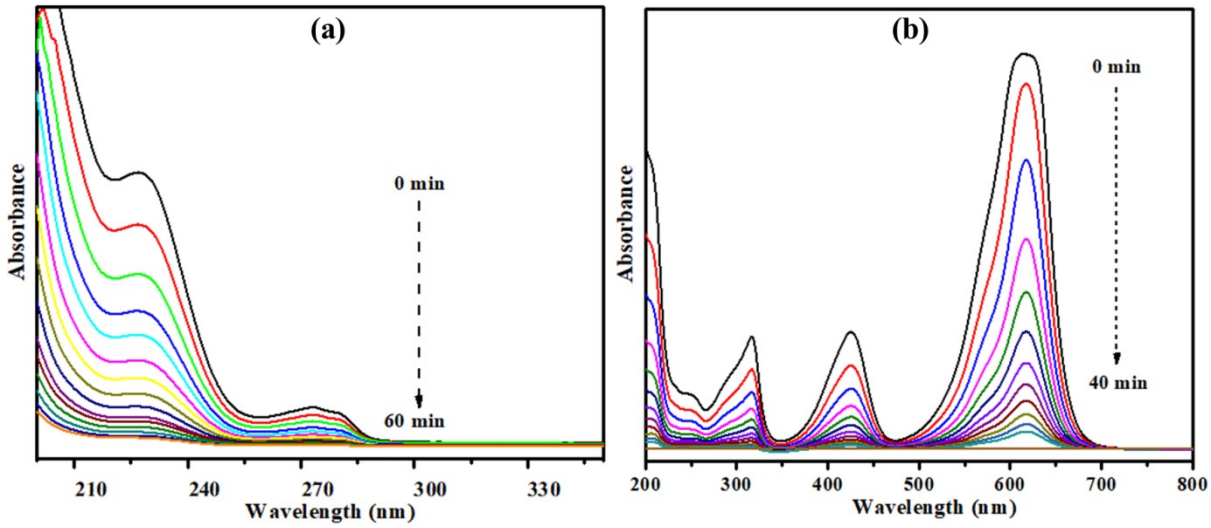

Fig. S9 UV–visible absorbance spectrum of photocatalytic degradation of a) AMX and b) MG vs irradiation time

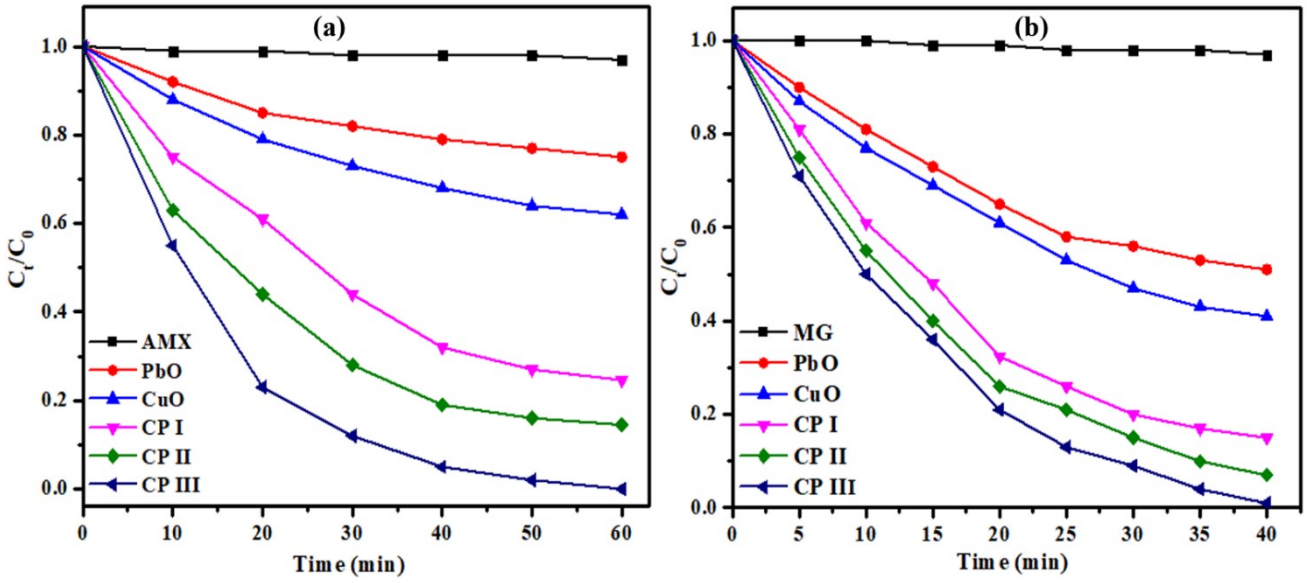

Fig. S10 a-b) Degradation kinetics of AMX and MG vs irradiation time

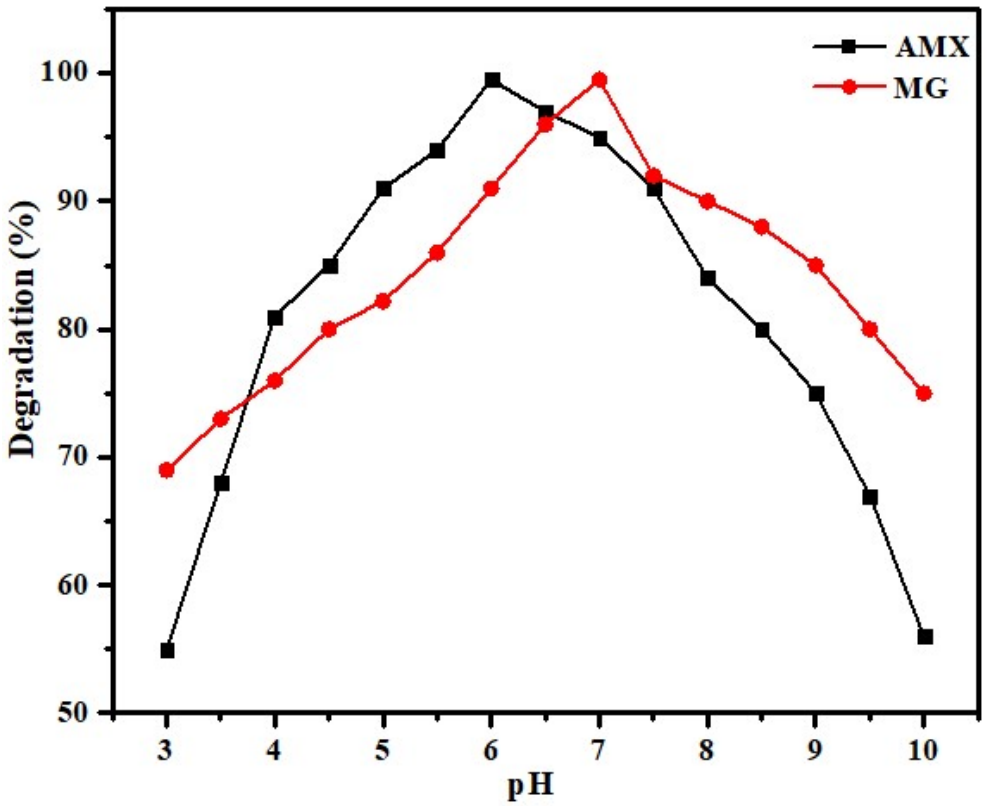

Fig. S11. Effect of pH value of solution on the AMX and MG pollutants photocatalysis

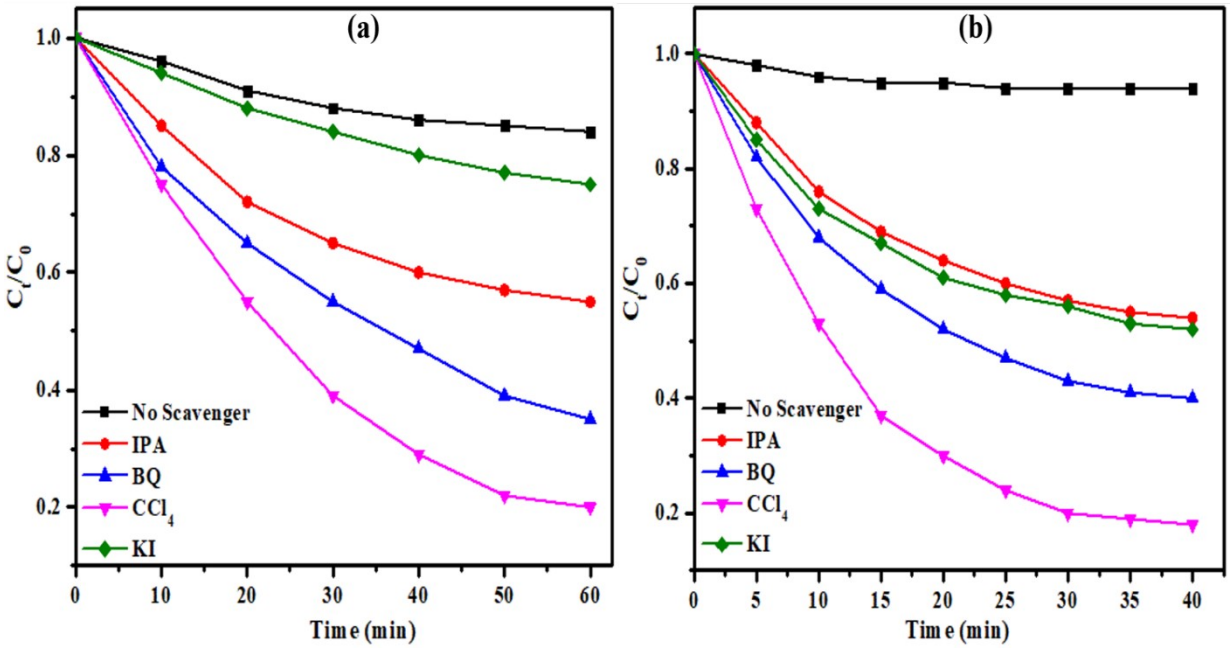

Fig. S12. Effect of scavengers on the change in concentration vs time for AMX and MG

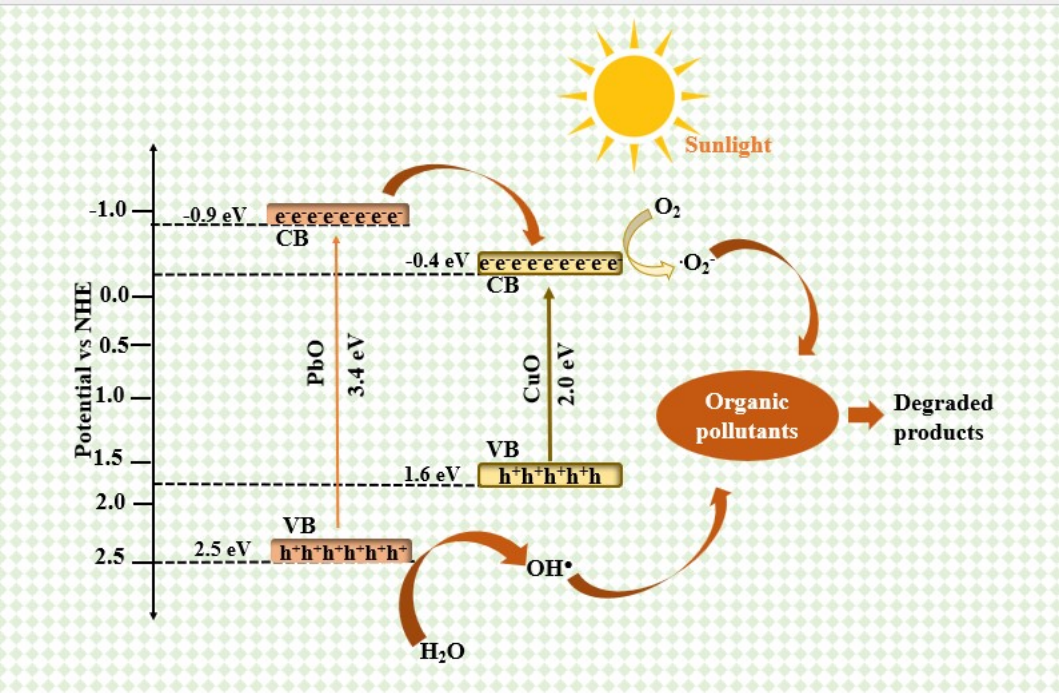

Fig. S13. A feasible strategy of the photocatalytic activity for antibiotic mineralization over CuO/PbO heterojunction

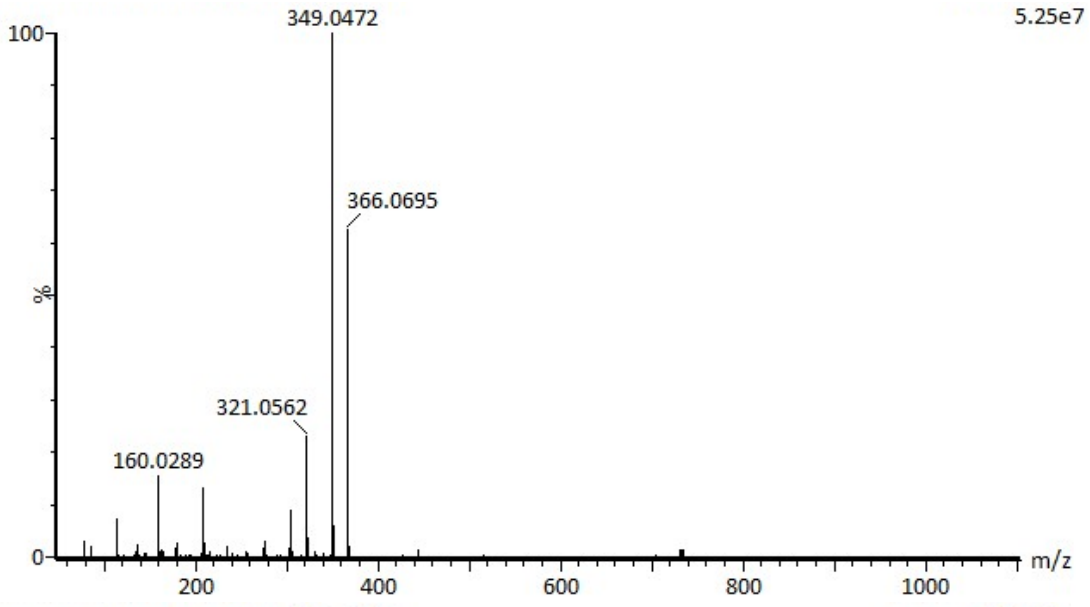
5.25e7
349.0472
366.0695
321.0562
160.0289
100
%
0
200
400
600
800
1000
m/z

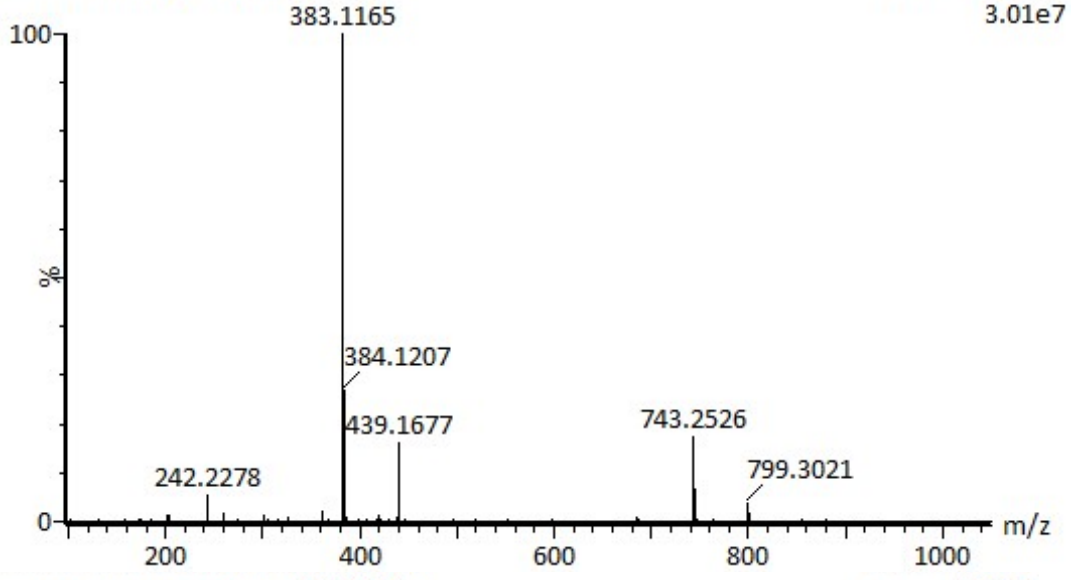
3.01e7
383.1165
384.1207
439.1677
743.2526
799.3021
242.2278
100
%
0
200
400
600
800
1000
m/z

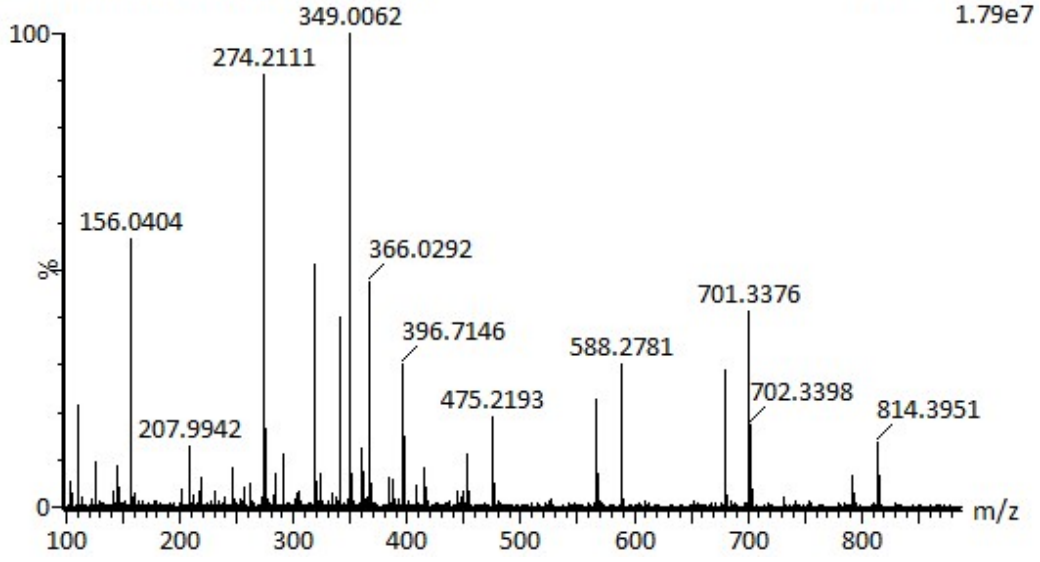
1.79e7
349.0062
274.2111
156.0404
366.0292
701.3376
396.7146
588.2781
475.2193
702.3398
814.3951
207.9942
100
%
0
100
200
300
400
500
600
700
800
m/z

Fig. S14. Various intermediates generated during AMX degradation by CuO/PbO heterojunction detected by LC-MS technique

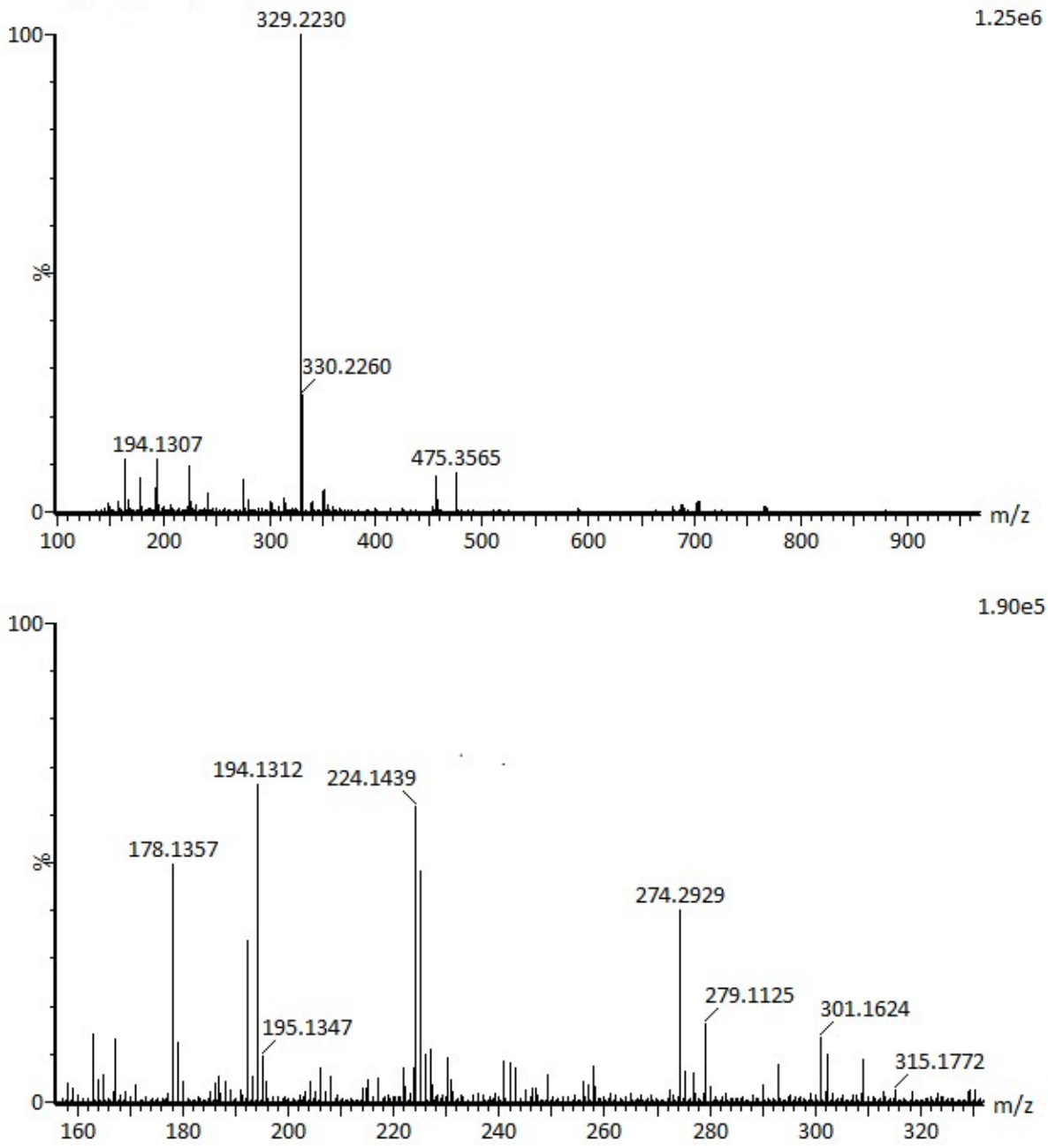

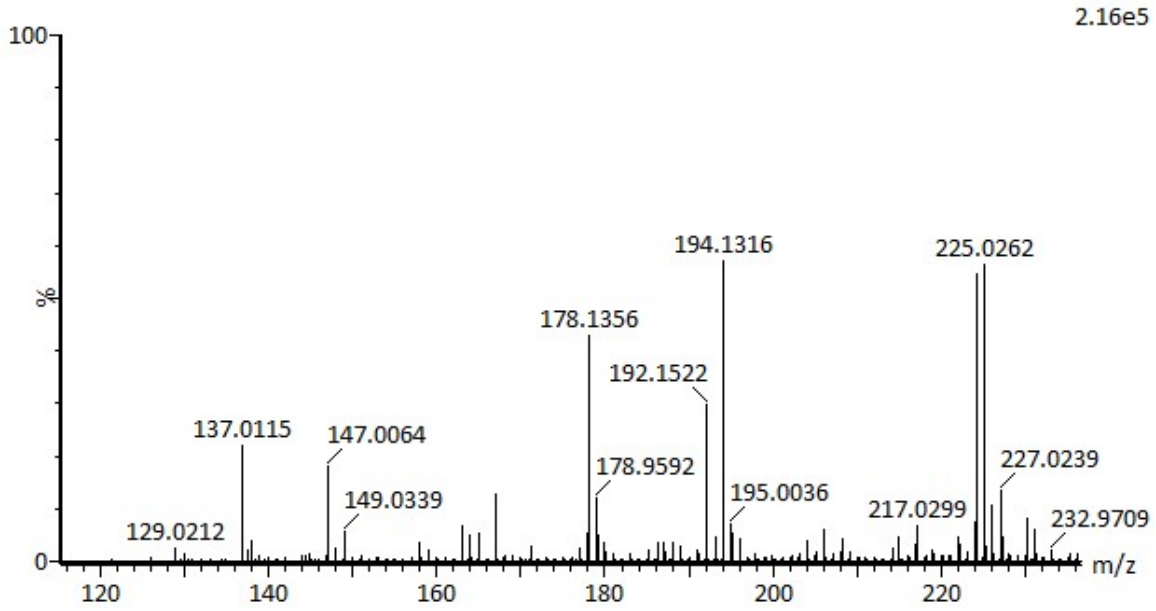

Fig. S15. Intermediates produced during MG dye degradation by CuO/PbO heterojunction detected by LC-MS

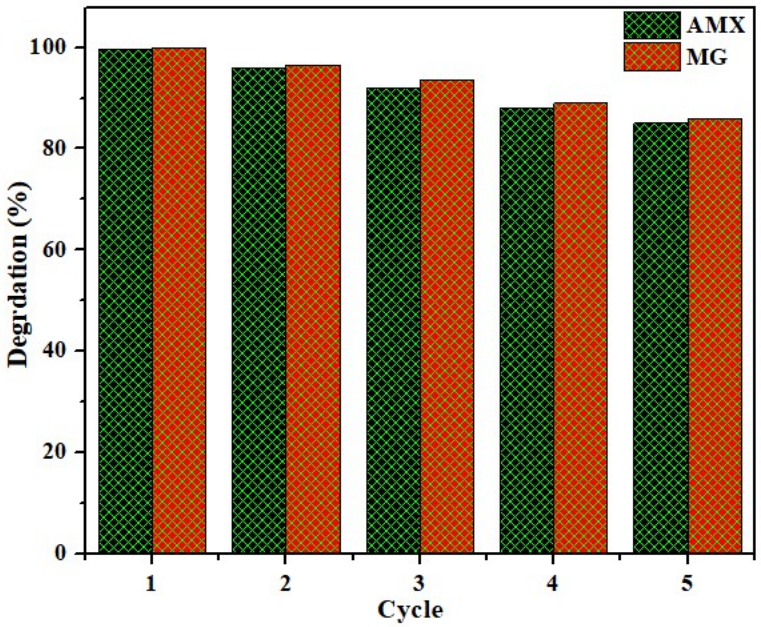

Fig. S16. Variation of degradation efficiency of the CuO/PbO heterojunction (CP-III) for AMX and MG dye over successive five cycles

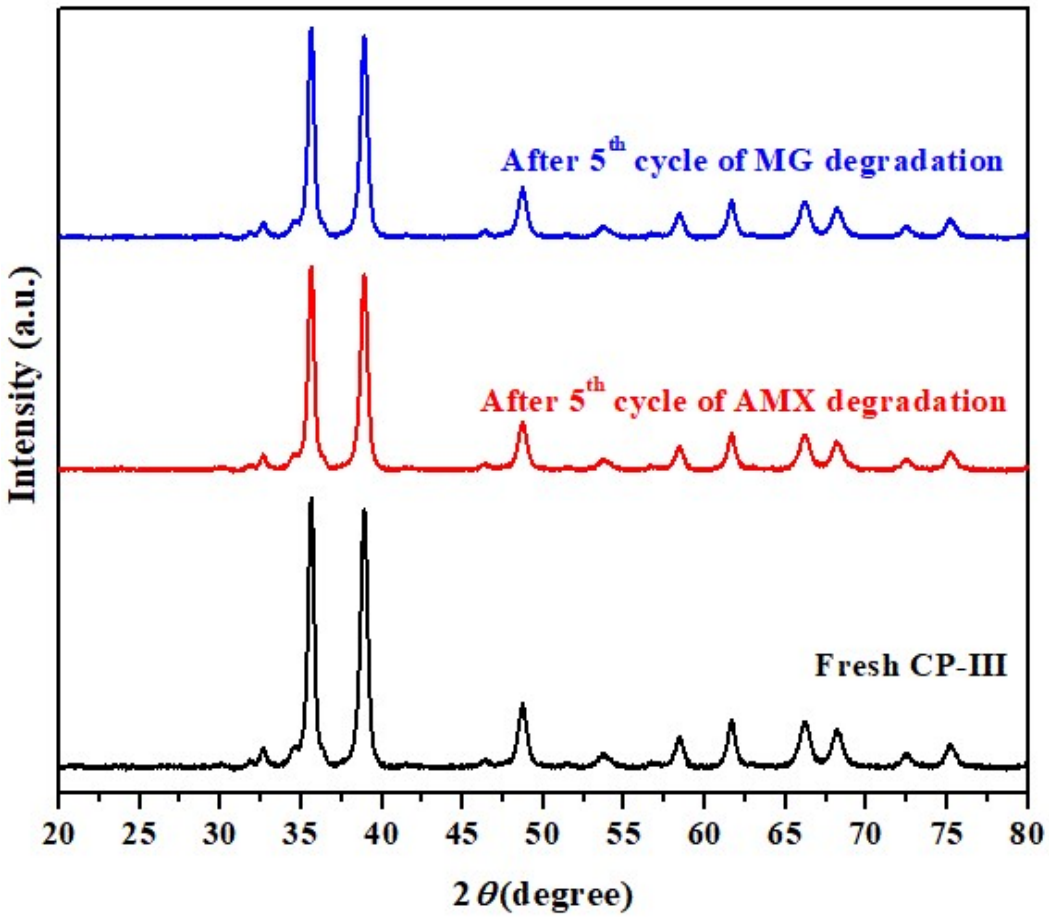

Fig. S17. XRD pattern of CZ III photocatalyst before and after 5 successive photocatalysis cycles